Journal of Materials Chemistry C

ELECTRONIC SUPPLEMENTARY INFORMATION

On the Asymmetric Evolution of the Optical Properties of a Conjugated Polymer during Electrochemical p- and n-type Doping

T. Lanz,[a] E. M. Lindh[a] and L. Edman[a,b]

a. Department of Physics, Umeå University, SE-90187 Umeå, Sweden
b. Corresponding author

1. Image of the experimental setup

Figure S1 displays a photograph of the experimental setup. A quartz cuvette is mounted on a 3D-printed support. The illumination beam (I_0) originating from the lamp, and the beam reflected off the device stack (I_R), are delivered from (and collected by) the first collimating lens. The illumination beam is transmitted through the front cuvette wall, the substrate, the transparent electrode, the Ph-PPV film under study, the electrolyte, and the back cuvette wall before being collected by the second collimating lens, which delivers the transmitted beam (I_T) to a spectrometer. The working electrode (WE) is pressed against the front cuvette wall with a custom-built steel spring, which also provides a connection to the potentiostat. The corresponding connections to the Ag pseudo-reference electrode (RE) and the Pt counter electrode (CE) are also indicated.

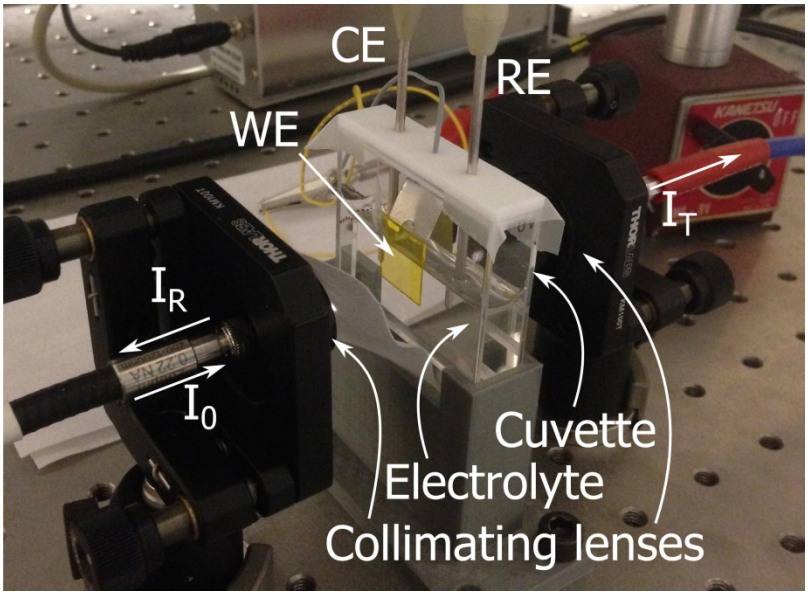

Figure S1. A photograph of the experimental setup. The different electrodes as well as the illumination, the reflected, and the transmitted beams are marked. In this particular experiment, the illumination beam was blocked by a piece of white fabric after the first collimating lens.

2. Data and Functions for the refractive index

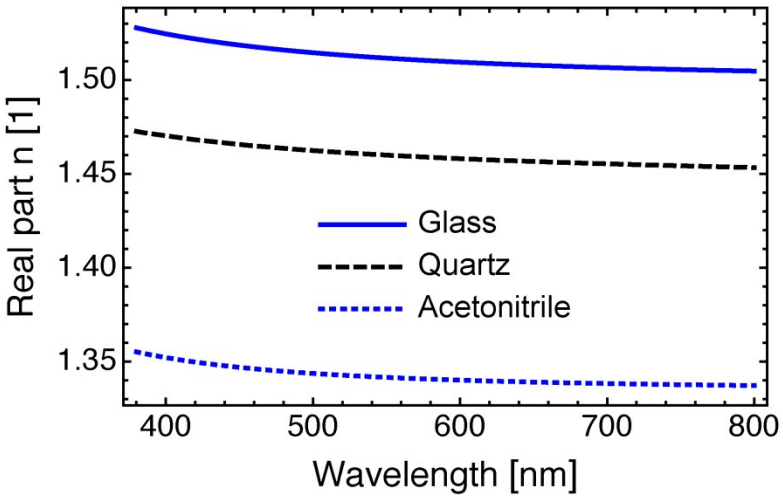

Figure S2. The real part of the refractive index for glass (data from vendor, Eagle XG, Corning) quartz,[1] and acetonitrile.[2] Note that the data for the electrolyte is estimated by that of acetonitrile on the virtue of that it is the dominating species in the electrolyte solution.

The data for the real part of the refractive index of the glass, quartz, and electrolyte materials in the spectroelectrochemistry setup (see Figure 1a) are presented in Figure S2. The imaginary part of the refractive index of these materials is set to zero, as they are all transparent in the visible range. The thicknesses of the different layers in the stack in Figure 1(a) are: d_{quartz} = 1.25 mm, d_{glass} = 0.8 mm, d_{ITO} = 145 nm, $d_{\text{electrolyte}}$ = 8.9 mm.

The complex dielectric function of ITO was parameterized by a linear combination of a Lorentz oscillator and a Drude oscillator:[3]

$$\varepsilon_{r,LD}(E) + i \cdot \varepsilon_{i,LD}(E) = \varepsilon_\infty + \frac{A_L}{E_L^2 - E^2 - i \cdot B_L E} + \frac{-A_D}{E^2 - i \cdot B_D E}, \tag{S1}$$

where n and k are obtained using $\varepsilon = (n + ik)^2$ and the Planck-Einstein relation $E = hc/\lambda$. The complex dielectric function of Ph-PPV was parameterized by

$$\varepsilon_{i,TL}(E) = \begin{cases} \dfrac{1}{E}\dfrac{AE_0C(E - E_g)^2}{\left(E^2 - E_g^2\right)^2 + C^2E^2}, & E > E_g \\ 0 & E < E_g \end{cases} \tag{S2}$$

$$\varepsilon_{r,TL}(E) = \varepsilon_r(\infty) + \frac{2}{\pi} P \int_{E_g}^{\infty} \frac{\zeta \cdot \varepsilon_i(\zeta)}{\zeta^2 - E^2} d\zeta, \tag{S3}$$

where P denotes the Cauchy principal value of the integral and can be expressed in closed form.[4]

3. Oscillator values

The refractive index dispersion of both p- and n-type doping of Ph-PPV can be described using a Tauc-Lorentz dispersion model as noted by Equations S2 and S3. Because the polaron transitions for the two doping types are located at different energies the corresponding additional oscillators also have different energies, which is manifested by separate sets of parameter values for p- and n-type doping. The doping concentrations and parameter values stated in Tables S1 and S2 are selected to be sufficient for reproducing the doping dependent refractive index dispersions shown in Figures 4 and 5 of the paper.

TABLE S1. Parameters of the Tauc-Lorentz model for p-type doped Ph-PPV.

σ_p [1/ru]	$\varepsilon(\infty)$	A_1 [eV]	C_1 [eV]	$E_{0,1}$ [eV]	$E_{g,1}$ [eV]	A_2 [eV]	C_2 [eV]	$E_{0,2}$ [eV]	$E_{g,2}$ [eV]
0.000	2.5	30.0	0.46	2.65	2.20	0.00	0.63	1.30	0.68
0.002	2.5	28.0	0.50	2.65	2.20	0.00	0.63	1.30	0.68
0.005	2.5	27.2	0.50	2.65	2.20	0.17	0.63	1.30	0.68
0.010	2.5	24.5	0.52	2.65	2.18	0.24	0.63	1.40	0.68
0.019	2.5	19.0	0.56	2.67	2.12	0.34	0.63	1.62	0.68
0.039	2.5	16.0	0.58	2.68	2.09	0.40	0.63	1.71	0.68
0.077	2.5	13.7	0.61	2.72	2.05	0.46	0.63	1.73	0.68
0.116	2.5	11.3	0.64	2.76	2.01	0.52	0.63	1.76	0.68
0.155	2.5	8.9	0.67	2.79	1.98	0.58	0.63	1.78	0.68
0.193	2.5	6.6	0.71	2.83	1.94	0.64	0.63	1.80	0.68

TABLE S2. Parameters of the Tauc-Lorentz model for n-type doped Ph-PPV.

σ_p [1/ru]	$\varepsilon(\infty)$	A_1 [eV]	C_1 [eV]	$E_{0,1}$ [eV]	$E_{g,1}$ [eV]	A_2 [eV]	C_2 [eV]	$E_{0,2}$ [eV]	$E_{g,2}$ [eV]
0.000	2.5	30.0	0.46	2.65	2.20	0.00	0.80	1.60	0.40
0.001	2.5	30.0	0.46	2.64	2.20	0.00	0.80	1.60	0.40
0.002	2.5	30.0	0.46	2.65	2.20	0.00	0.80	1.60	0.40
0.048	2.5	30.0	0.47	2.63	2.20	0.00	0.80	1.60	0.40
0.097	2.5	26.1	0.49	2.62	2.20	0.07	0.80	1.60	0.40
0.193	2.5	21.8	0.51	2.60	2.20	0.21	0.80	1.60	0.40
0.290	2.5	17.8	0.53	2.59	2.20	0.34	0.80	1.60	0.40
0.386	2.5	16.4	0.55	2.59	2.20	0.34	0.80	1.60	0.40
0.483	2.5	15.2	0.55	2.59	2.20	0.34	0.80	1.60	0.40
0.579	2.5	14.1	0.55	2.59	2.20	0.35	0.80	1.60	0.40

4. Mass density of Ph-PPV

The mass density of Ph-PPV films was measured by a relative transmittance method[5]. Four Ph-PPV films were fabricated on glass substrates (14.8 x 14.8 mm^2) using the procedure described in the experimental section. After drying, corner beads and irregular edges were carefully removed with a razor blade so that a uniform and well-defined film was remaining on the substrate. The film thickness was measured by contact-profilometry at 9 different locations, while the area was measured by image analysis of photographs. This allowed for a calculation of the volume of the film.

Each film was then dissolved in 10 ml of toluene (the complete dissolution was verified by that the remaining substrates featured no photoluminescence) to produce a set of "sample solutions". A set of "reference solutions" with different concentrations were prepared by dissolving a carefully measured mass of Ph-PPV in toluene. Both the sample and reference solutions were optically clear. Their integrated transmittance in the wavelength region between 430–470 nm (where Ph-PPV is strongly absorbing but where its photoluminescence is zero) was measured with a spectrometer. With the aid of Beer-Lambert's law:

$$T(c) = T(0)\exp(-\alpha d c), \quad \text{(S4)}$$

where $T(0)$ is the transmittance of the optical system at zero Ph-PPV concentration, α is the molar attenuation coefficient of Ph-PPV, d is the optical path length (= 10 mm), and c is the mass concentration of Ph-PPV in the solution, it was possible to establish $T(0)$ and α from a log-plot of the reference-solution data. It was thereafter a straightforward task to derive values for c for the

sample solutions, and to calculate the mass density of Ph-PPV by simply dividing the established mass with the measured volume. Measurement data and derived values for the density are presented in Table S3. The mean and standard deviation of the 9 measurements on samples 2, 3, and 4 (sample 1 was discarded as an outlier) are 1.03(9) g/cm^3. Although the uncertainty in this measurement is significant, our results indicate that the employed estimate of 1 g/cm^3 is reasonable.

TABLE S3. Data for the measurement of Ph-PPV mass density. Values extracted from the transmittance measurements are shown in italic, and numbers within parenthesis represent the standard deviation of three measurements.

	$\log(\int T d\lambda)$ [a.u.]†	Concentration [g/ml]·10^{-6}	Dry film volume [cm^3]·10^{-5}	Mass [g]·10^{-5}	Mass density [g/cm^3]
Ref. 1	3.497(1)	0.6234	‡	‡	‡
Ref. 2	3.286(3)	2.475	‡	‡	‡
Sample 1	3.331(9)	2.09(8)	1.487	2.09(8)	1.41(5)
Sample 2	3.408(5)	1.44(4)	1.486	1.44(4)	0.97(3)
Sample 3	3.365(5)	1.81(4)	1.570	1.81(4)	1.15(2)
Sample 4	3.413(3)	1.40(3)	1.437	1.40(3)	0.97(2)

† This is the logarithm of the integrated (430–470 nm) transmittance.
‡ Not available

References

1. I. H. Malitson, *J Opt Soc Am*, 1965, **55**, 1205-&.
2. K. Moutzouris, M. Papamichael, S. C. Betsis, I. Stavrakas, G. Hloupis and D. Triantis, *Appl Phys B-Lasers O*, 2014, **116**, 617-622.
3. S. D'Elia, N. Scaramuzza, F. Ciuchi, C. Versace, G. Strangi and R. Bartolino, *Appl Surf Sci*, 2009, **255**, 7203-7211.
4. G. E. Jellison and F. A. Modine, *Applied Physics Letters*, 1996, **69**, 371-373.

